


 Cite this: *RSC Adv.*, 2025, **15**, 38811

## Release study of microplastic fibres and heavy metals from disposable surgical face masks in aqueous medium: the effect of physio-chemical factors and shear forces

 Soupam Das,<sup>a</sup> Anjali Shaw,<sup>a</sup> M. R. Sumaiya,<sup>b</sup> J. B. Jeeva<sup>b</sup> and Amitava Mukherjee  <sup>a</sup>

Since the COVID-19 pandemic broke out, there has been a dramatic surge in the usage of disposable face masks, and even though the pandemic has passed, discarded masks persist in aquatic systems where they continue to release microplastic fibres. These masks are composed of plastic nonwoven fabrics and can potentially contribute polypropylene (PP) microplastics to the environment. This investigation aimed to assess the potential for these PP microplastics to be released into the water by disposable surgical face masks under different parameters. This study systematically assesses various factors that may affect the release of microplastic fibres into the natural aquatic environment. The initial investigation focused on the impact of various hydro-chemical parameters, including pH levels (4, 7, and 9), ionic strength (IS) at 10, 50, and 100 mM, and humic acid (HA) concentrations (0.1, 1, and 10 mg L<sup>-1</sup>), to analyse the overall release pattern of microplastic fibres from facemasks. The experimental findings demonstrate that pH, ionic strength, and humic acid significantly influenced the release pattern of the fibres, with the highest release observed at pH 9, 10 mM IS, and 0.1 mg L<sup>-1</sup> HA. At higher IS and HA concentrations, the release of microplastic fibres was lower compared to that at lower concentrations. This study also emphasises the impact of varying shear stress levels on the release dynamics of fibres and co-contaminants like heavy metals (HMs) from disposable surgical facemasks over different time intervals. Furthermore, the release pattern of the microplastic fibres was examined in various natural water systems, including lakes and seawater. Future studies will extend this work to longer exposure durations to better capture the long-term release dynamics of microplastic fibres from masks.

 Received 21st August 2025  
 Accepted 10th October 2025

DOI: 10.1039/d5ra06197k

[rsc.li/rsc-advances](http://rsc.li/rsc-advances)

### 1. Introduction

Throughout the COVID-19 pandemic, masks were essential to everyday life, serving as the most effective barrier against respiratory illnesses.<sup>1</sup> Regardless of the increasing removal of legal mandates for mask-wearing in public spaces by most nations, individuals are nonetheless urged to continue using masks to enhance personal hygiene and mitigate the risk of viral transmission. Despite standardised protocols for the disposal of masks by governments and organisations, a significant quantity is improperly discarded by the general population. Environmental concerns over disposable surgical face masks are increasing because of the substantial amounts of masks that have been carelessly discharged into various water bodies during and after the COVID-19 outbreak. These disposed-used facemasks may serve as a source of microplastics

(MPs), nanoplastics (NPs), and other secondary pollutants or co-contaminants.

After extensive research, polypropylene (PP) polymers have been identified as the primary leachates emitted from disposable face masks, potentially expediting the process by environmental weathering.<sup>2</sup> In deionised (DI) water under agitation, disposable face masks have been seen to emit micro/nano plastic particles/fibres, heavy metals (such as Pb, Cd, and Se), and organic contaminants, with predominating PP polymers.<sup>3</sup> In numerous instances, a range of chemicals, such as plasticisers and flame retardants, were routinely incorporated into polymers to improve the characteristics of the materials.<sup>4</sup> Furthermore, the degradation and fragmentation of polypropylene demonstrate sensitivity to photodegradation, thermal exposure, and ambient oxygen.<sup>5</sup> Regrettably, most of these investigations were performed in DI water under simulated physical circumstances. The impact of water conditions, namely waters with varying chemical solutes, has seldom been examined.<sup>6</sup>

The degradation of disposed masks occurs through natural processes, including wind, water, and ultraviolet exposure,

<sup>a</sup>Centre for Nanobiotechnology, Vellore Institute of Technology, Vellore, India. E-mail: amitav@vit.ac.in; amit.mookerje@gmail.com

<sup>b</sup>Sensor and Biomedical Technology, School of Electronics Engineering, Vellore Institute of Technology, Vellore, India



resulting in alterations to their physical and chemical characteristics and the subsequent release of microplastics into the ecosystem.<sup>7</sup> The original polymer's surface exhibits increased roughness due to weathering, resulting in heightened fragility and an increased propensity to form small chips.<sup>8,9</sup> It is essential to acknowledge that mechanical abrasion caused by water and sediments can significantly influence weathering.<sup>10</sup> According to Chen *et al.*, (2021),<sup>11</sup> masks emit more microfibers when subjected to underwater conditions and the ageing process. Wang *et al.*, (2021)<sup>12</sup> indicated that the quantity released from the middle layer surpasses that of both the inner and outer layers.

To closely replicate the conditions under which discarded masks might release microplastics in the environment, we subjected commercially available single-use disposable surgical masks to a range of typical external factors, including fluctuations in pH, ionic strength, and differing concentrations of humic acid. The release of microplastics from masks was assessed within a 90-min timeframe following exposure to various parameters. We analysed the release kinetics of microplastics and heavy metals emitted from the masks. Furthermore, the underlying factors contributing to the variation in the release potential of microplastic fibres were determined by examining the mask's surface morphology using FTIR and Raman spectroscopy. The experiments were carried out to investigate the release of microplastics from masks under various physiochemical parameters. In addition, heavy metals present in the leachate were also analysed using ICP-OES. Data were gathered to substantiate the potential for microplastic and co-contaminant release under differing environmental conditions, thereby offering a theoretical framework for understanding the environmental impact associated with the improper disposal of masks after the pandemic.

## 2. Materials and methods

### 2.1. Materials

Disposable surgical face masks have been purchased from local pharmacy shops. The masks are 16.5 by 9 cm in size. Fig. S1 shows that the mask was blue. The masks were undamaged, and they were still within their expiration date. Analytical grade extra pure sodium chloride (NaCl) was acquired from SRL India Pvt. Ltd (CAS Number 7617-14-5). Humic acid was procured from Sigma-Aldrich (CAS Number 14808-60-7). The mechanical geared stirrer used for agitation was acquired from REMI India. All experimental experiments used ultrapure distilled water (18.2 MΩ cm at 25 °C) from Pall Corporation, Ann Arbor, Michigan, USA.

### 2.2. Preparation of humic acid stock solution

Humic acid (100 mg L<sup>-1</sup>) stock was prepared in double distilled water (pH 7). The solution was subjected to a rotary shaker for 24 h to assure complete dissolution. The solution was filtered using a 0.45 µm membrane filter to exclude particle debris. A TOC Analyzer (TOC-L, Shimadzu) was used to ascertain the total organic carbon content of the produced stock solution, which

was confirmed to be 100 mg L<sup>-1</sup>. The stock solution was serially diluted to achieve its intended working concentrations of 0.1, 1, and 10 mg L<sup>-1</sup>.

### 2.3. Microplastic release experiments in the presence of pH, ionic strength, and humic acid

The study aimed to establish whether shear force facilitates or impedes the release of microplastic fibres from face masks under various physiochemical parameters. The release experiments were investigated at different pH (4, 7, and 9), ionic strengths (10, 50, and 100 mM), and humic acid concentrations (0.1, 1, and 10 mg L<sup>-1</sup>). Three pH values (4, 7, and 9) were selected to represent acidic, neutral, and alkaline conditions commonly encountered in natural waters. Reported pH values of rivers and lakes typically fall between 4–9, influenced by acid rain, carbonate buffering, and biological activity.<sup>39</sup> A recent study on microplastic degradation was conducted at pH 3, 7, and 11, which are similar to the pH values used in our study.<sup>46</sup> NaCl was used as the model electrolyte, with concentrations of 10, 50, and 100 mM. These NaCl concentrations approximate the ionic strengths of low-mineral-content freshwater (~10 mM), moderately mineralised rivers or groundwater (~50 mM), and estuarine waters (up to ~100 mM).<sup>40</sup> HA concentrations of 0.1, 1, and 10 mg L<sup>-1</sup> were selected to represent natural levels of dissolved organic matter. These values are consistent with the dissolved organic carbon content reported in lakes and rivers worldwide.<sup>41</sup> Moreover, the chosen ionic strength and humic acid concentrations were based on values reported in previous literature on microplastic transport and degradation.<sup>47</sup>

A mask was fragmented and placed into the distilled water glass beaker. The pH of water was adjusted to acidic or basic ranges using 0.1 N HCl or NaOH solution. Additionally, the ionic strength of water was modified by adding 10, 50, or 100 mM NaCl solutions. The original humic acid stock solution was diluted by serial dilution to reach the desired working concentrations of 0.1, 1, and 10 mg L<sup>-1</sup>. A geared stirrer was positioned in the centre of each glass beaker to simulate the effect of shear stress on the fibre release pattern. Rotational rates of 150 and 400 rpm were selected to replicate the slow and fast flows found in natural water bodies with 150 and 400 rpm corresponding to a flow velocities of ~0.23 m s<sup>-1</sup> and ~1.26 m s<sup>-1</sup> respectively.<sup>13</sup> Distinct experiments were performed for 15, 30, 45, 60, 75, and 90 min, respectively as this study was designed as a short-term investigation. Since microplastic fibres from face masks are expected to continue releasing over time without a clear end-point, the focus here was not on long-term release but rather on capturing the short-term dynamics within a controlled timeframe. The characteristics and duration chosen for the research adhere to the international norms outlined in OECD test guideline (TG) No. 318.<sup>14</sup> While guideline (TG) No. 318 applies formally to nanomaterials, here we used its agitation and medium-selection framework as methodological inspiration to evaluate the initial release phase of mask fibres and leachates over 90 min.<sup>45</sup> Previous literature has shown that this guideline has primarily been applied to nanomaterials,<sup>51</sup> and in our study, it served as a reference



framework. This shorter timeframe was chosen to capture early-stage detachment processes prior to significant chemical ageing, and to provide a baseline reference for subsequent longer-term studies. Different pH levels, ionic strength, natural organic matter (humic acid), and a comparative examination of microplastic fibre and heavy metal release under dynamic stresses could strengthen understanding of the leachate release pattern from masks.

#### 2.4. Microplastic release experiments in environmental water samples

Experiments were performed to examine the release patterns of microplastic fibres from face masks in freshwater and marine environments to simulate environmental conditions. Lake water as a freshwater medium was collected from VIT Lake, Vellore, Tamil Nadu, India. The lake water was passed through various filtration methods and sterilised before being used for the experimental purpose.<sup>15</sup> Natural seawater as a marine water medium was collected from Rameshwaram, Tamil Nadu, India. Our previous studies have mentioned seawater filtration and sterilisation.<sup>16</sup> The physicochemical characteristics of the environmental water samples are shown in Table S1. Mask pieces were added to each environmental water sample in a glass beaker, and shear stresses were applied as described in the experimental section.

#### 2.5. Quantification and identification of the leached microplastics

Microplastics in DSFML released at various time intervals (15, 30, 45, 60, 75, and 90 min) were counted by observation under an optical microscope (Leica DM 2500). The leachate samples were filtered using a 0.45 µm nitrocellulose membrane filter. The filter paper was dried and examined under an optical microscope to count the fibres. We developed a precise MATLAB algorithm to count the microplastic fibres visible in the microscopic images accurately.<sup>17</sup>

The microscopic images are read from their respective directories and individually processed to extract only the microscopic data. A threshold value is calculated for each image to binarise it. This process is repeated for all images. The microfibres are then identified by analysing their connected components, and each particle is labelled and counted. Refer to Fig. S2 for the flowchart detailing the algorithm used to write the MATLAB code.

Fourier-transform infrared (FTIR) spectroscopy was used to thoroughly examine the surface chemical groups in the leachate samples. The dried fibres on the filter paper were analysed by high-precision FTIR equipment (IR Spirit; Shimadzu, Japan) and compared to plastic standards provided by the reference library.<sup>17</sup> The study was performed at 15-min intervals for up to 90 min to observe any spectral variations. We performed carbonyl index (CI) and hydroxyl index (HI) variation analyses to assess the photo-oxidative breakdown of microplastics from face masks. The CI and HI were calculated by the ratios of the absorbance peaks from FTIR at 1718 and 3340 cm<sup>-1</sup> relatives to the peak at 974 cm<sup>-1</sup>, respectively.

Raman spectroscopy was conducted to ascertain the microplastics released from the leachates. The fibres on the filter paper were dried and analysed using Raman spectroscopy (wavelength: 785 nm; spectral range: 300 to 3200 cm<sup>-1</sup>) (Anton Paar, Cora 5001, Austria). The classification of plastic kinds was determined by comparing the acquired spectra to the specified standards in the library database.<sup>11</sup>

Inductively coupled plasma-optical emission spectrometry (ICP-OES) was utilised to identify heavy metals in nFML. Before analysis, a 3 kDa membrane filter paper was used to separate the microplastic fibres from the leachate solution. The filtered solution underwent ICP-OES analysis.

#### 2.6. Quality assurance and control

All sampling and analytical equipment were thoroughly cleaned in the laboratory using sterile deionized water. During sampling, clean gloves and cotton lab coats were worn. Glassware was acid-washed, rinsed with Milli-Q water, and heat-treated at 400 °C to remove residual organic contaminants. To minimize microplastic contamination, all tools and containers were made of metal or glass. Additionally, the investigators avoided any contact with materials similar to those used in the mask.

#### 2.7. Statistical analysis

All experiments in this research were conducted thrice. The data sets are displayed as the average value and the standard deviation, indicating the measure of variability. The graphs were computed using GraphPad Prism version 8.0.

### 3. Results and discussion

#### 3.1. Influence of various environmental factors on the release of microplastic fibres from face masks

**3.1.1. Influence of pH.** Fig. 1 displays optical microscopic images of DSFML released at different pH after 90 min. Irregularly shaped microplastic fibres measuring between  $1 \pm 0.3$  and  $100 \pm 2.1$  µm were observed from the microscopic images. Our previous research showed similar-sized microplastic fibre released from face masks.<sup>18-20</sup> In contrast, prior research by Li *et al.*, (2021)<sup>21</sup> indicated that traditional masks often have bigger plastic fibres, ranging from 600 to 1800 µm. Fig. 4A and B illustrate the number of microplastic fibres released at various time intervals under various shear stresses (150 and 400 rpm, respectively) and at different pH levels (4, 7, and 9). Examination using a Matlab program on the microscopic pictures revealed a gradual increase in the concentration of plastic fibres released into the leachate over time. At 0th min microplastic fibres were not observed under the microscope. The lowest concentration was observed at 15 min, followed by steady increases, resulting in the maximum concentration at 90 min (Table S8). The findings indicate that the most extensive fibre release occurred at pH 4, followed by pH 7 and 9 (Fig. 4A and B). In addition, high shear stress (400 rpm) (Fig. 4B, D and F) led to an increased release of fibres compared to reduced shear stress (150 rpm) (Fig. 4A, C and E). As the environment got more acidic



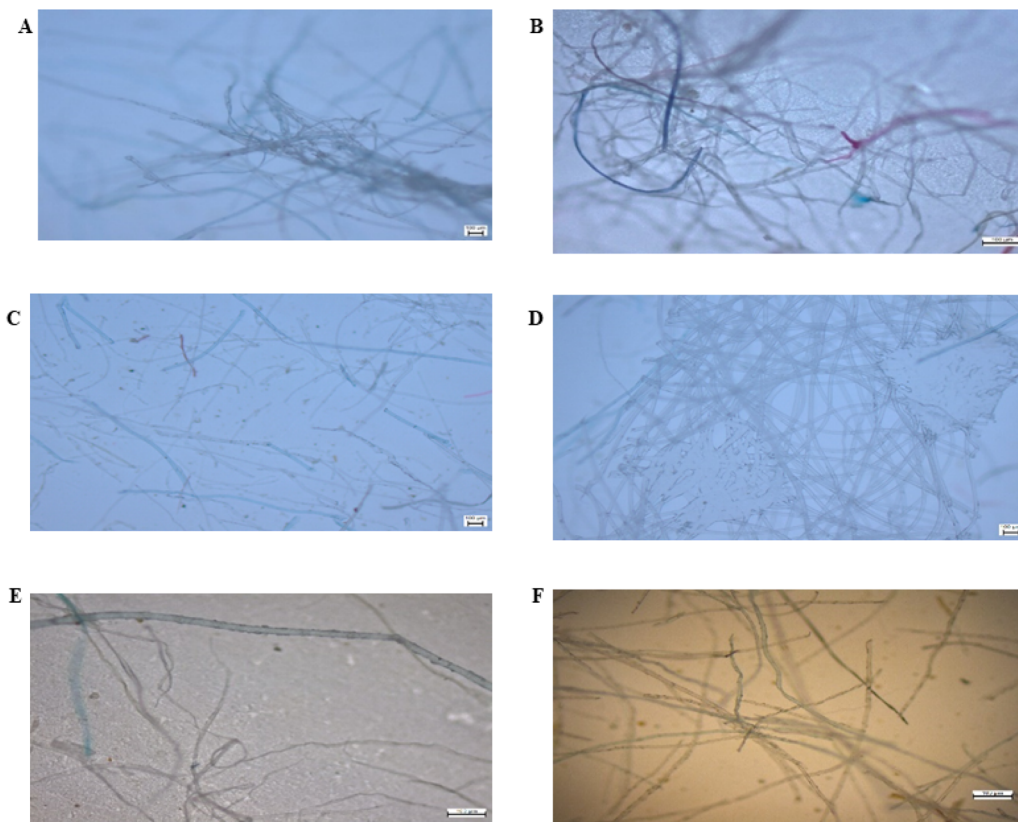


Fig. 1 Microscopic images of microplastic fibres released from DSFML after 90 min at various pH (A) pH 4 150 rpm (B) pH 7 150 rpm (C) pH 9 150 rpm (D) pH 4 400 rpm (E) pH 7 400 rpm (F) pH 9 400 rpm.

(pH 4–7), a higher quantity of MP fibres was released. Both acidic and alkaline environments seemingly facilitated MP release, presumably due to the polymer's backbone being susceptible to attack by  $\text{OH}^-$  ions in alkaline environments and  $\text{H}_3\text{O}^+$  ions in acidic ones. The hydrolysis of O–C–N bonds in the polypropylene substance used in the mask was also a significant component<sup>22</sup> moreover, smaller fibres and particles ( $\leq 100 \mu\text{m}$ ) were more abundant in the acidic environment. Nevertheless, pH influences surface charge and the ionisation state of functional groups, which may weaken hydrogen bonding at fibre junctions. Under acidic or alkaline conditions, this can facilitate the detachment of loosely bound surface fibres, explaining the higher counts observed despite minimal chemical ageing.<sup>42</sup> Previous researchers also observed a similar phenomenon, where the number of microplastic fibres released from the mask decreased with an increase in pH from 3 to 7, corroborating our results.<sup>23</sup>

Fig. S3 displays the FTIR spectra of microplastic fibres released from DSFML at various time intervals (15, 30, 45, 60, 75, and 90 min), at differing pH levels (4, 7, and 9), and at two different shear forces (150 and 400 rpm). The detected bands at all-time intervals validated the existence of polypropylene groups, as corroborated by comparison with a reference spectral library. Raman spectroscopy confirmed the identification of polypropylene in the released microplastics, exhibiting a 98% similarity index relative to the Raman spectra reference library

(Fig. S4). Prior research has established the FTIR and Raman attributes of polypropylene microplastics originating from surgical disposable face masks.<sup>5,17,24</sup>

The FTIR spectra at various intervals, across all pH conditions and shear stresses, increased intensity at  $1718 \text{ cm}^{-1}$  and  $3340 \text{ cm}^{-1}$ , corresponding to carbonyl and hydroxyl groups, respectively. Fig. 5A and B depicted the CI variations of the leachate under different pH values (Table S12). This indicates a gradual rise in these functional groups, signifying the improved breakdown of polypropylene fibres during leaching. The increase in carbonyl content with time was inconsistent, corroborating earlier research.<sup>25</sup> The HI values exhibited a progressive rise from 1.010 at 15 min to 1.034 at 90 min, paralleling the pattern in the CI index, indicating that the extent of ageing did not inherently escalate with prolonged exposure (Fig. 6A and B) (Table S16). This may be ascribed to the potent inhibitory effects of antioxidant additives and the development of oxygen-containing surface functional groups.<sup>6</sup> Though the CI and HI values have increased but the overall variation remains low during the 15–90 min exposure, and the Raman and FTIR spectra revealed no new characteristic peaks. This stability reflects the chemical robustness of polypropylene backbones over short timescales, even under acidic or alkaline conditions.<sup>37</sup> However, fibre counts increased markedly with higher shear (400 rpm) compared to lower shear (150 rpm), indicating that hydrodynamic agitation accelerates physical detachment



while the underlying chemical structure remains unchanged. Thus, short-term release under varying pH is dominated by shear-induced fibre mobilisation rather than chemical ageing.<sup>48</sup>

Elemental analysis of DSFML revealed that trace quantities of heavy metals were leached for both the shear stresses, *i.e.* 150 rpm (Table S2) and 400 rpm (Table S3). The results indicate that only negligible amounts of Cd, Cr, Cu, Ni, and Zn were released. A recent research by<sup>26</sup> discovered that masks immersed in freshwater for seven days emitted inorganic chemicals, including B, Al, Ti, Fe, Cu, and Sr. The disparity in released components between the previous research and the current one may be ascribed to variations in mask composition and the release medium.<sup>3</sup> similarly indicated that the emission of heavy metals and compounds from surgical masks may fluctuate depending on parameters such as mask composition, time of exposure, and the release medium.

**3.1.2. Influence of ionic strength.** Fig. 2 represents optical microscopic images of microplastic fibres in DSFML, released at various ionic strengths under two different shear stresses. Fibre sizes ranging from  $1 \pm 0.6$  to  $100 \pm 2.6 \mu\text{m}$  can be observed. The number of microplastic fibres released at multiple time intervals under different ionic strengths (10, 50, and 100 mM) and at various shear stresses (150 and 400 rpm) are shown in Fig. 4C and D, respectively. Using the Matlab program, a gradual increase in the concentration of microplastic fibres was observed to be released into the leachate over time. The lowest

concentration level was observed at 15 min, followed by steady increases, resulting in the maximum concentration at 90 min (Table S9). The findings indicate that the most extensive fibre release occurred at 10 mM, followed by 50 mM and 100 mM salt concentrations. Furthermore, elevated shear stress (400 rpm) (Fig. 2B, D and F) led to an increased release of fibres compared to reduced shear stress (150 rpm) (Fig. 2A, C and E). NaCl can corrode plastics, but only to some extent. The melt-blown fibres were inadequately bonded during the melt-blowing process. Nonetheless, interaction with the NaCl solution could lead to the separation of fibres, and polymer composites are also adversely affected by the ageing impact of saline water on their mechanical characteristics. It can be hypothesised that immersion in saline solutions might damage the integrity of the fibre network within DFM, consequently leading to an increased release of microplastics.<sup>10,23,27</sup> Noted a contrasting trend; with an increase in ionic strength, there was a corresponding increase in the release of microplastic fibres from surgical masks. Elevated ionic strength reduces electrostatic repulsion between polymer surfaces and surrounding colloids, promoting closer contact and mechanical separation.<sup>43</sup> This effect likely explains the observed increase in detached fibres, even in the absence of detectable chemical transformation. Previous investigations indicated that the distinctive melt-blown method used for the mask's intermediate layer

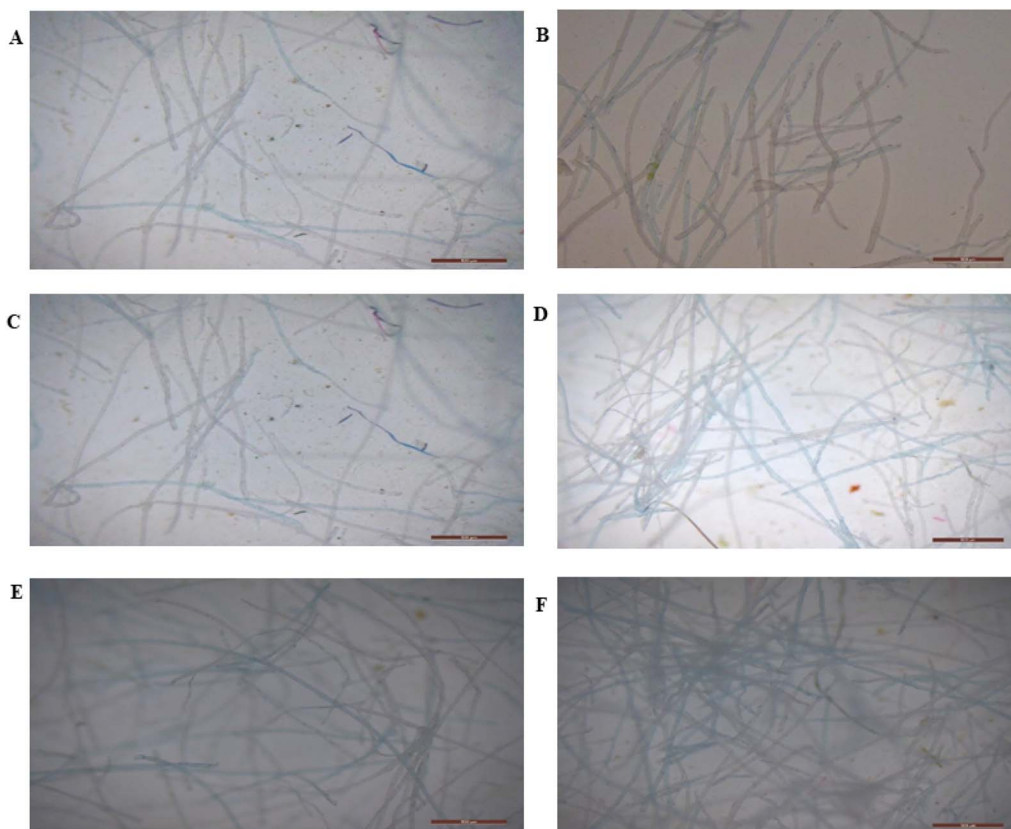


Fig. 2 Microscopic images of microplastic fibres released from DSFML after 90 min at various ionic strengths (A) IS 10 mM 150 rpm (B) IS 50 mM 150 rpm (C) IS 100 mM 150 rpm (D) IS 10 mM 400 rpm (E) IS 50 mM 400 rpm (F) IS 100 mM 400 rpm.



enhanced filtering effectiveness but also resulted in significant emissions of microplastics.<sup>28,29</sup>

Fig. S5 shows the FTIR spectra of microplastic fibres released from DSFML at various time intervals (15, 30, 45, 60, 75, and 90 min) at differing NaCl concentrations (10, 50, and 100 mM) and shear forces (150 and 400 rpm). The detected spectral bands of the microplastic fibres released at different intervals confirmed the presence of polypropylene groups by comparing them with a reference spectral library. The intensity of the FTIR spectral bands was also found to increase slightly over time. Raman spectroscopy also confirmed the identification of polypropylene in the released microplastics, exhibiting a 96.9% similarity index relative to the Raman spectra reference library (Fig. S6).

The FTIR spectra at various intervals, across all ionic strength conditions and shear stresses, increased intensity at  $1718\text{ cm}^{-1}$  and  $3340\text{ cm}^{-1}$ , corresponding to carbonyl and hydroxyl groups, respectively. Similar to the pH parameter, the increase in carbonyl content with time was inconsistent (Fig. 5C and D) (Table S13). Also, the HI values exhibited a progressive rise from 15 min to 90 min, paralleling the pattern in CI (Fig. 6C and D), indicating that the extent of ageing did not inherently escalate with prolonged exposure (Table S17). Ionic strength primarily influenced the dispersion and detachment of fibres, with higher counts consistently detected under stronger agitation (400 rpm). These experimental results confirm that NaCl concentration modulates the physical stability of the

microplastic fibres in the suspension, while shear force dictates the rate of their release, and neither factor produced measurable oxidation of polypropylene within the experimental timeframe.<sup>38</sup>

Elemental analysis of DSFML revealed that trace quantities of heavy metals leached from the masks (Table S4 and S5). The results indicate that only insignificant amounts of Cd, Cr, Cu, Ni, Pb and Zn were released under both the shear stresses (150 and 400 rpm). Minute differences in heavy metal concentrations between 150 and 400 rpm of shear stresses were observed.

**3.1.3. Influence of humic acid concentrations.** In the natural environment, HA constitutes about 50% of dissolved organic matter as a complexly organised polyelectrolyte molecule.<sup>30</sup> Fig. 3 displays optical microscopic images of microplastic fibres in DSFML, released at various HA concentrations under two different shear stresses (150 and 400 rpm). Here also. The fibre sizes ranging within  $100 \pm 3.6\text{ }\mu\text{m}$  can be observed. The number of microplastic fibres released at various time intervals under different HA concentrations (0.1, 1, and  $10\text{ mg L}^{-1}$ ) and at various shear stresses (150 and 400 rpm) are shown in Fig. 4E and F, respectively. Using the MATLAB program, we observed a gradual increase in the concentration of microplastic fibres was observed to be released into the leachate over time. The lowest concentration level was observed at 15 min, followed by steady increases, resulting in the maximum concentration at 90 min (Table S10). The findings indicate that

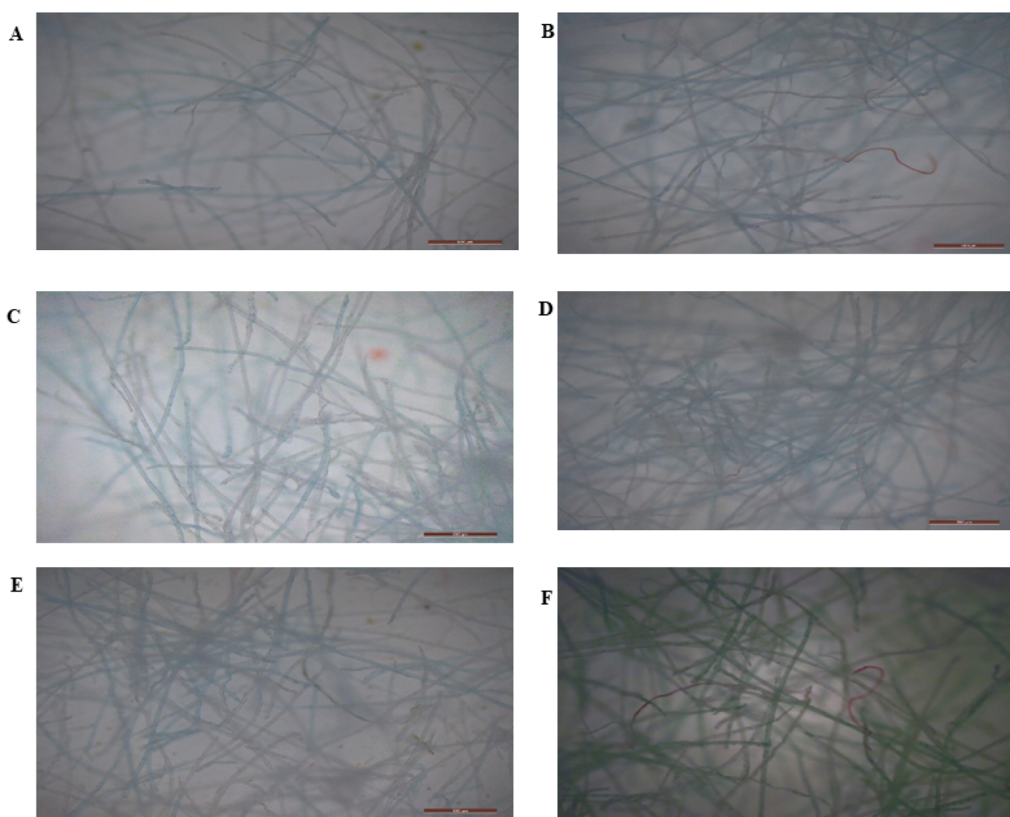


Fig. 3 Microscopic images of microplastic fibres released from DSFML after 90 min at various humic acid concentrations (A) HA  $0.1\text{ mg L}^{-1}$  150 rpm (B) HA  $1\text{ mg L}^{-1}$  150 rpm (C) HA  $10\text{ mg L}^{-1}$  150 rpm (D) HA  $0.1\text{ mg L}^{-1}$  400 rpm (E) HA  $1\text{ mg L}^{-1}$  400 rpm (F) HA  $10\text{ mg L}^{-1}$  400 rpm.



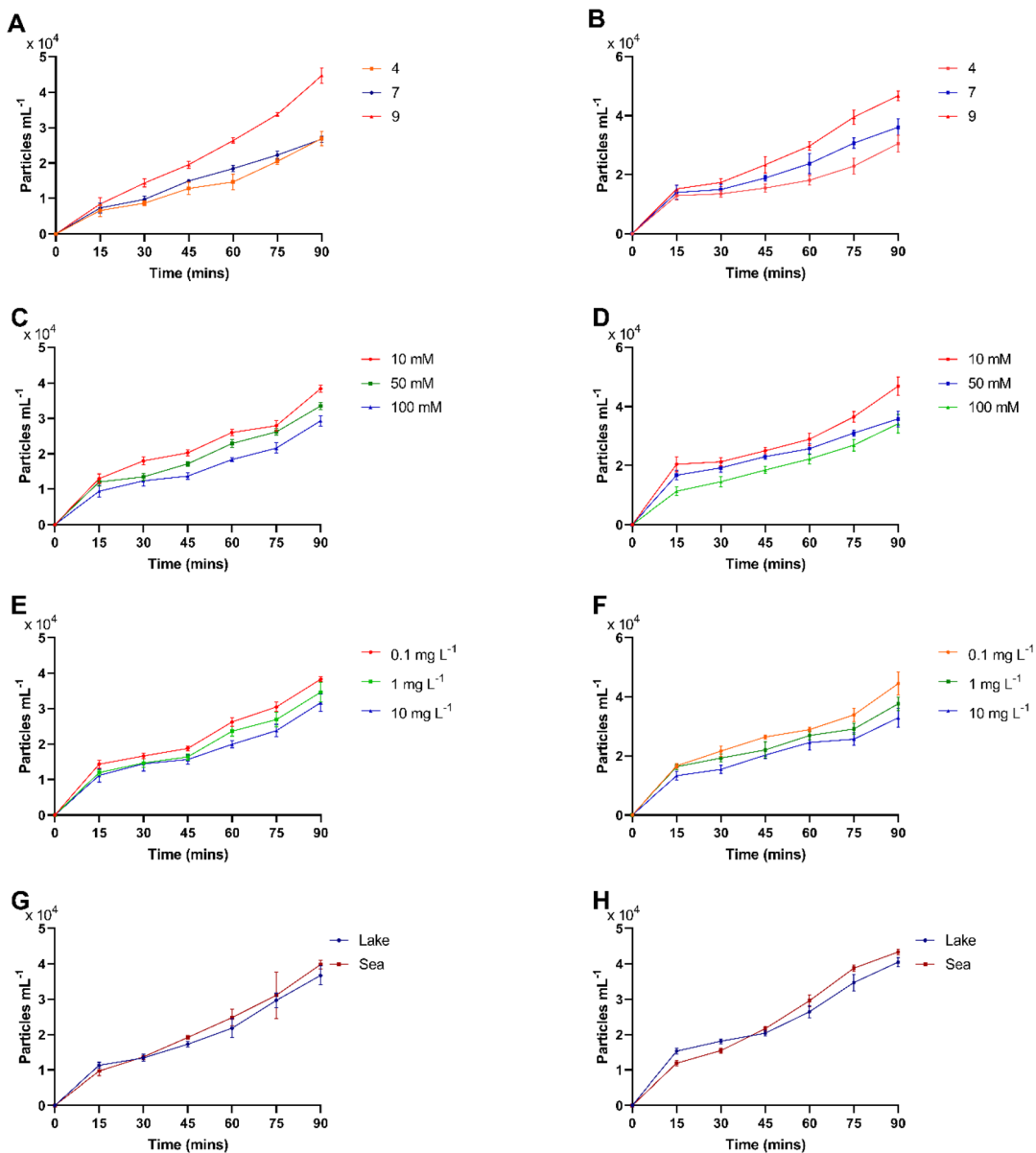


Fig. 4 Concentration of microplastic fibres released at different time points under shear forces at different physio-chemical factors (A) pH-150 rpm (B) pH-400 rpm (C) IS-150 rpm (D) IS-400 rpm (E) HA-150 rpm (F) HA-400 rpm (G) environmental water-150 rpm (H) environmental water-400 rpm.

the most extensive fibre release occurred at  $10 \text{ mg L}^{-1}$ , followed by  $1 \text{ mg L}^{-1}$  and  $0.1 \text{ mg L}^{-1}$  of HA concentrations. Furthermore, elevated shear stress (400 rpm) led to an increased release of fibres (Fig. 3B, D and F) compared to reduced shear stress (150 rpm) (Fig. 3A, C and E). The presence of natural organics ( $0.1\text{--}10 \text{ mg L}^{-1}$ ) enhanced fibre release relative to DI water. Humic acid molecules can adsorb onto polypropylene surfaces, modifying surface hydrophobicity and providing steric stabilisation that prevents re-aggregation.<sup>44</sup> These interactions favour the physical dispersion of released fibres, though they did not trigger detectable chemical modification during the experimental window. Previous researchers also observed similar HA effects on microplastic fibre release from masks.<sup>23</sup> They noted a strong correlation between high HA content and the release of

microplastic fibres from the mask. HA facilitated the release of MPs from the masks. Fibre MPs mostly ranged in size from 100 to 500  $\mu\text{m}$  and 500 to 1000  $\mu\text{m}$ , although finer fibres ( $\leq 100 \mu\text{m}$ ) were seldom observed. The administration of HA produced a somewhat acidic environment. Concurrently, HA could improve the movement of MPs by amplifying electrostatic and steric repulsion. MPs exhibited a negative charge in the natural environment, and the surface potential of released MPs may become more negative with higher concentrations of HA.<sup>31</sup>

Fig. S7 displays the FTIR spectra of microplastic fibres released from DSFML at various time intervals (15, 30, 45, 60, 75, and 90 min) at differing HA concentrations (0.1, 1, and  $10 \text{ mg L}^{-1}$ ) and shear forces (150 and 400 rpm). The detected bands at all-time intervals validated the existence of

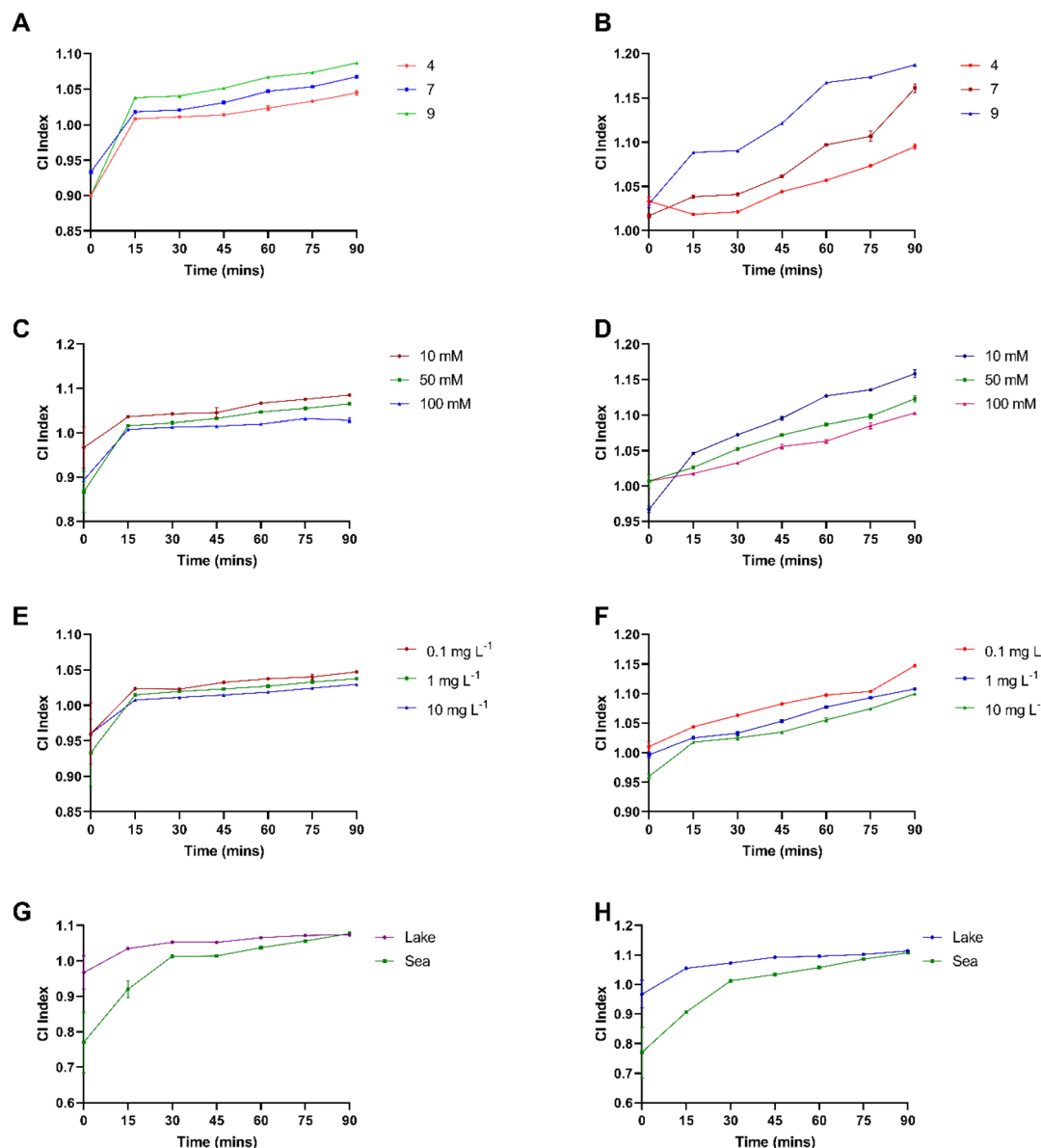


Fig. 5 CI variation at different time points under shear forces at different physio-chemical factors (A) pH-150 rpm (B) pH-400 rpm (C) IS-150 rpm (D) IS-400 rpm (E) HA-150 rpm (F) HA-400 rpm (G) environmental water-150 rpm (H) environmental water-400 rpm.

polypropylene groups, as corroborated by comparison with a reference spectral library. The intensity of the FTIR spectral bands was also found to increase slightly over time. Raman spectroscopy confirmed the identification of polypropylene in the released microplastics, exhibiting a 96.9% similarity index relative to the Raman spectra reference library (Fig. S8).

The FTIR spectra at various intervals, across all HA concentrations and shear stresses, increased intensity at  $1718\text{ cm}^{-1}$  and  $3340\text{ cm}^{-1}$ , corresponding to carbonyl and hydroxyl groups, respectively. Similar to the pH parameter, the increase in carbonyl content with time was inconsistent (Fig. 5E and F) (Table S14). Also, the HI values exhibited a progressive rise from 15 min to 90 min, paralleling the pattern in CI (Fig. 6E and F), indicating that the extent of ageing did not inherently escalate with the given exposure (Table S18). This was mainly because

HA can change the surface roughness of the PP-made masks, thereby increasing the oxygen-containing functional groups on its surface.<sup>32</sup> Our previous study showed increased CI and HI values when N95 face masks interacted with lake water having natural organics.<sup>20</sup> Natural organics likely enhanced fibre release through surface interactions, with pronounced increases in particle counts especially under higher shear.<sup>49</sup> Yet, even in the presence of natural organic matter and strong agitation, the chemical indices remained stable, reinforcing that short-term exposure mobilises fibres physically but does not trigger detectable chemical transformation of the polymer.<sup>50</sup>

Elemental analysis of DSFML revealed that trace quantities of heavy metals leached from the masks (Table S6 and S7). The results indicate that only minute amounts of Cd, Cr, Cu, Ni, Pb and Zn were released under both the shear stresses (150 and 400



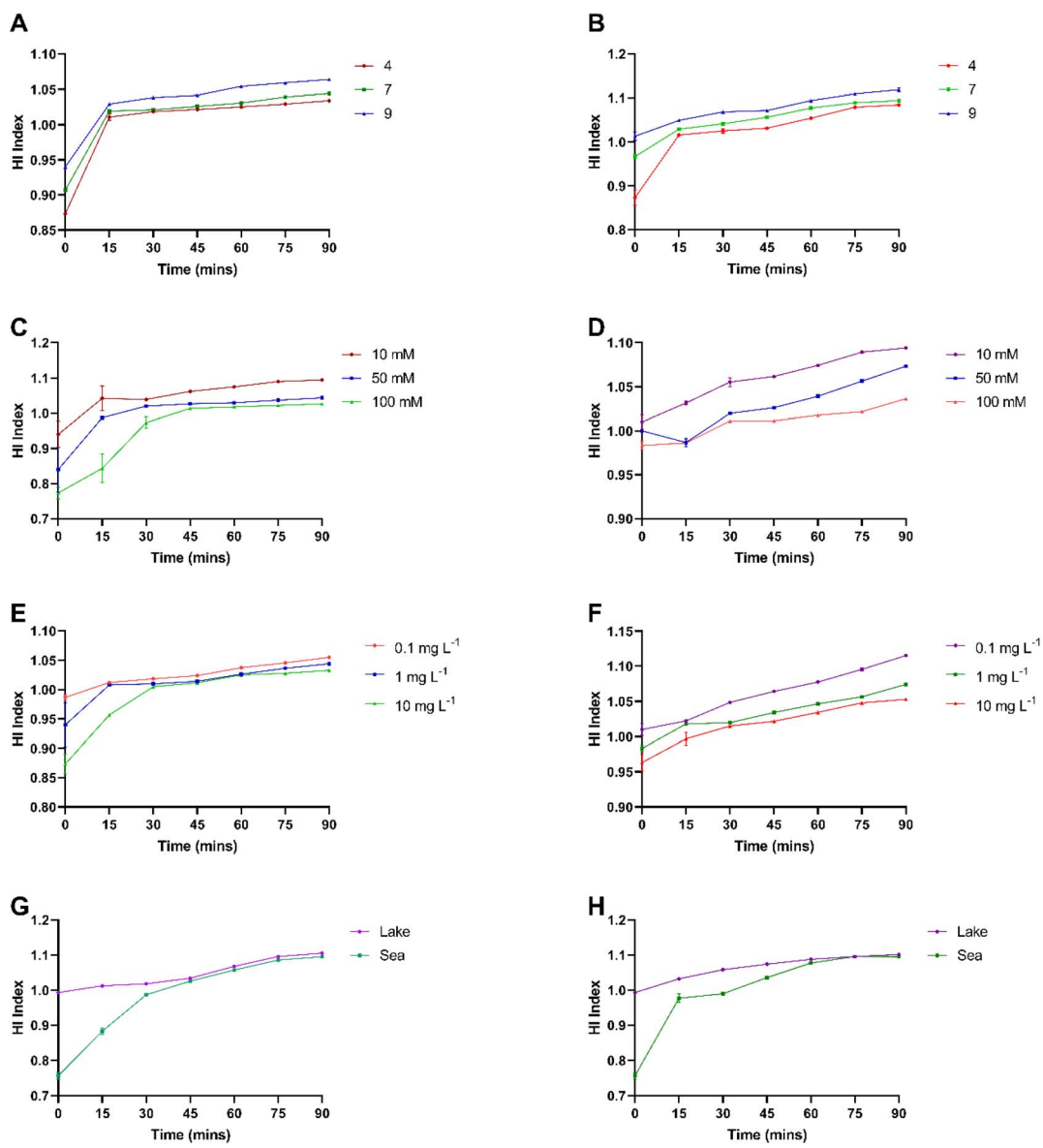


Fig. 6 HI variation at different time points under shear forces at different physio-chemical factors (A) pH-150 rpm (B) pH-400 rpm (C) IS-150 rpm (D) IS-400 rpm (E) HA-150 rpm (F) HA-400 rpm (G) environmental water-150 rpm (H) environmental water-400 rpm.

rpm) similar to the conditions of pH and ionic strengths. Minute differences in heavy metal concentrations were observed between 150 and 400 rpm of shear stresses.

### 3.2. Release behaviour of microplastics from face masks in different environmental waters

The time-dependent release of microplastic fibres under varying shear stresses (150 and 400 rpm) across two different environmental waters (Lake and Sea water) is illustrated in Fig. S9. The highest microplastic fibres were released in the lakewater, followed by Sea water. Additionally, it was observed that applying high-shear stress (400 rpm) results in a more significant release of fibres from the mask compared to low-shear stress (150 rpm) (Table S11). Similarly, the CI and HI indices also increase over time, indicating greater degradation of microplastic fibres from the masks. In a lake water environment, factors like pH and

natural organics can influence the release of microplastic fibres from the masks. Previous research indicates that face masks might emit many microplastics, even in freshwater ecosystems like lake water.<sup>7,33</sup> The release of PP into the lake water was much greater than that in seawater. Generally, lake water had much more organic carbon than other natural water sources, which may be attributable to high humus content. Lakes often get a more significant input of organic matter from adjacent terrestrial sources, such as decomposing flora and fauna, while the open ocean exhibits a more diluted dispersion of organic matter owing to its extensive volume.<sup>34,35</sup> The increased release of PP plastic fibres in lake water compared to seawater may be attributed to weathering from chemical oxidation.<sup>36</sup> On the other hand, lake waters showed elevated pH levels compared to seawater, perhaps accelerating the breakdown and release of microfibers, resulting in a proliferation of smaller plastic fibres.

Our previous research reported microplastic fibres released in lake water from disposable surgical face masks.<sup>18,19</sup>

## 4. Conclusion and limitations

This study assessed the release pattern of leachates from disposable surgical face masks in an aqueous medium, including essential environmental physicochemical parameters. Incorporating natural organic matter into the water system and modifying pH levels increased the concentration of microplastic fibres in the leachates. The principal results of this work demonstrate that humic acid-induced repulsive forces stabilised leachate release, leading to an increased concentration of fibres in the leachate. Moreover, it may be inferred that salt content was also a significant factor influencing the release of PP microplastic fibres. An increased release of microplastic fibres in the leachate was seen at high ionic strengths. Moreover, shear stresses were exerted at low and high stirring velocities to replicate the natural dynamic aquatic systems. Elevated shear stresses enhance the release of microplastic fibres in the leachates. It should be noted that this study was conducted using a single type of commercially available surgical mask in order to maintain consistency across experiments. However, variations in mask type and brand, including differences in polymer composition, additives, and manufacturing processes, may influence both the concentration and composition of released microplastics and heavy metals. Consequently, the release pattern observed in this work may differ from those associated with other mask types, and future studies should consider inter-brand and inter-type comparisons to capture this variability more comprehensively. It is essential to acknowledge that this study's results, computations, and analytical methods are contingent and only relevant to waters with similar characteristics. To better understand the leachate release behaviour from face masks in aquatic environments, this behaviour may be investigated over extended durations in large-scale aquatic systems.

## Author contributions

Soupam Das: investigation, methodology, visualization, formal analysis, writing original draft; Anjali Shaw: investigation, methodology, formal analysis; Sumaiya M. R.: software, formal analysis, data curation; Jeeva J. B.: software, formal analysis, data curation, resources, writing- review and editing; Amitava Mukherjee: conceptualization, methodology, supervision, project administration, writing- review and editing.

## Conflicts of interest

There are no conflicts to declare.

## Data availability

The main text and the supplementary information (SI) contains all the data. Supplementary information is available. See DOI: <https://doi.org/10.1039/d5ra06197k>.

## Acknowledgements

We acknowledge the assistance of the inductively coupled plasma-optical emission spectrometry facility at IIT Madras. This work was supported by the Council of Scientific & Industrial Research (CSIR), Ministry of Science & Technology, Govt. of India (File No.-09/0844(18217)/2024-EMR-I).

## References

- 1 J. Ahmed, A. Harker and M. Edirisinghe, *Med. Devices Sens.*, 2020, **3**, e10120.
- 2 H. Du, S. Huang and J. Wang, *Sci. Total Environ.*, 2022, 152980.
- 3 G. L. Sullivan, J. Delgado-Gallardo, T. Watson and S. Sarp, *Water Res.*, 2021, **196**, 117033.
- 4 A. Bodaghi, *Polym. Adv. Technol.*, 2020, **31**, 355–367.
- 5 A. Jemec Kokalj, A. Dolar, D. Drobne, M. Marinšek, M. Dolenc, L. Škrlep, G. Strmljan, B. Mušič and A. S. Škapin, *Microplast. Nanoplast.*, 2022, **2**, 1–15.
- 6 L. Liu, H. Ma and B. Xing, *Chemosphere*, 2024, **349**, 140976.
- 7 T. A. Aragaw, *Mar. Pollut. Bull.*, 2020, **159**, 111517.
- 8 Y. K. Song, S. H. Hong, M. Jang, G. M. Han, S. W. Jung and W. J. Shim, *Environ. Sci. Technol.*, 2017, **51**, 4368–4376.
- 9 Y. Sun, J. Yuan, T. Zhou, Y. Zhao, F. Yu and J. Ma, *Environ. Pollut.*, 2020, **265**, 114864.
- 10 P. Wu, J. Li, X. Lu, Y. Tang and Z. Cai, *Sci. Total Environ.*, 2022, **806**, 150458.
- 11 X. Chen, X. Chen, Q. Liu, Q. Zhao, X. Xiong and C. Wu, *Environ. Pollut.*, 2021, **285**, 117485.
- 12 Z. Wang, C. An, X. Chen, K. Lee, B. Zhang and Q. Feng, *J. Hazard. Mater.*, 2021, **417**, 126036.
- 13 B. Lv, C. Wang, J. Hou, P. Wang, L. Miao and B. Xing, *Environ. Pollut.*, 2020, **257**, 113584.
- 14 OECD, Test No. 318: Dispersion Stability of Nanomaterials in Simulated Environmental Media, *OECD Guidelines for the Testing of Chemicals, Section 3*, OECD Publishing, Paris, 2017, DOI: [10.1787/9789264284142-en](https://doi.org/10.1787/9789264284142-en).
- 15 S. Das, V. Thiagarajan, N. Chandrasekaran, B. Ravindran and A. Mukherjee, *Comp. Biochem. Physiol., Part C: Toxicol. Pharmacol.*, 2022, 109305, DOI: [10.1016/j.cbpc.2022.109305](https://doi.org/10.1016/j.cbpc.2022.109305).
- 16 C. Rex M and A. Mukherjee, *Environ. Sci. Pollut. Res.*, 2023, **30**, 122700–122716.
- 17 J. Ma, F. Chen, H. Xu, H. Jiang, J. Liu, P. Li, C. C. Chen and K. Pan, *Environ. Pollut.*, 2021, **288**, 117748.
- 18 S. Das, N. Chandrasekaran and A. Mukherjee, *Comp. Biochem. Physiol., Part C: Toxicol. Pharmacol.*, 2023, 109587.
- 19 S. Das and A. Mukherjee, *Environ. Sci.: Processes Impacts*, 2023, **25**, 1428–1437.
- 20 S. Das, S. M R, J. B. Jeeva and A. Mukherjee, *Chemosphere*, 2024, **363**, 142851.
- 21 H. Li, H. Chen, J. Wang, J. Li, S. Liu, J. Tu, Y. Chen, Y. Zong, P. Zhang and Z. Wang, *Front. Microbiol.*, 2021, **12**, 717272.
- 22 B. K. H. Lim and E. San Thian, *Sci. Total Environ.*, 2022, **813**, 151880.
- 23 H. Jiang, J. Su, Y. Zhang, K. Bian, Z. Wang, H. Wang and C. Wang, *Chemosphere*, 2022, **309**, 136748.



- 24 G. E. De-la-Torre, D. C. Díoses-Salinas, C. I. Pizarro-Ortega, M. D. Fernández-Severini, A. D. Forero-López, S. Dobaradaran and R. Selvasembian, *J. Hazard. Mater. Adv.*, 2023, 100326.
- 25 J. Almond, P. Sugumaar, M. N. Wenzel, G. Hill and C. Wallis, *e-Polym.*, 2020, **20**, 369–381.
- 26 M. Sendra, P. Pereiro, M. P. Yeste, B. Novoa and A. Figueiras, *J. Hazard. Mater.*, 2022, **428**, 128186.
- 27 M. V. Kini and D. Pai, *Mater. Today: Proc.*, 2022, **52**, 689–696.
- 28 J. Delgado-Gallardo, G. L. Sullivan, M. Tokaryk, J. Russell, G. Davies, K. Johns, A. Hunter, T. Watson and S. Sarp, *ACS ES&T Water*, 2022, **2**, 527–538.
- 29 J. Sun, S. Yang, G.-J. Zhou, K. Zhang, Y. Lu, Q. Jin, P. K. Lam, K. M. Leung and Y. He, *Environ. Sci. Technol. Lett.*, 2021, **8**, 1065–1070.
- 30 S. Shabbir, M. Faheem, A. A. Dar, N. Ali, P. G. Kerr, Z.-G. Yu, Y. Li, S. Frei, G. Albasher and B. S. Gilfedder, *Chemosphere*, 2022, **293**, 133515.
- 31 H. Rong, M. Li, L. He, M. Zhang, L. Hsieh, S. Wang, P. Han and M. Tong, *J. Hazard. Mater.*, 2022, **426**, 127787.
- 32 H. Luo, C. Liu, D. He, J. Sun, A. Zhang, J. Li and X. Pan, *Water Res.*, 2022, **222**, 118921.
- 33 U. Cabrejos-Cerdeña, G. E. De-la-Torre, S. Dobaradaran and S. Rangabhashiyam, *J. Hazard. Mater.*, 2023, **443**, 130273.
- 34 G. M. Ward, A. K. Ward, C. N. Dahm and N. G. Aumen, in *The Biology of Particles in Aquatic Systems*, CRC press, 2nd edn, 2020, pp. 45–73.
- 35 S. E. Findlay, in *Fundamentals of Ecosystem Science*, Elsevier, 2021, pp. 81–102.
- 36 J. Duan, N. Bolan, Y. Li, S. Ding, T. Atugoda, M. Vithanage, B. Sarkar, D. C. Tsang and M. Kirkham, *Water Res.*, 2021, **196**, 117011.
- 37 G. Zhang, C. Nam, T. M. Chung, L. Petersson and H. Hillborg, Polypropylene copolymer containing cross-linkable antioxidant moieties with long-term stability under elevated temperature conditions, *Macromolecules*, 2017, **50**(18), 7041–7051.
- 38 R. Asoodeh, *Stability and Aggregation of Microplastics Suspended in Aqueous Media*, Doctoral dissertation, Memorial University of Newfoundland, 2024.
- 39 T. A. Clair and A. Hindar, Liming for the mitigation of acid rain effects in freshwaters: a review of recent results, *Environ. Rev.*, 2005, **13**(3), 91–128.
- 40 M. Leira, R. Meijide-Failde and E. Torres, Diatom communities in thermo-mineral springs of Galicia (NW Spain), *Diatom Res.*, 2017, **32**(1), 29–42.
- 41 H. E. Mengchang, S. H. I. Yehong and L. I. N. Chunye, Characterization of humic acids extracted from the sediments of the various rivers and lakes in China, *J. Environ. Sci.*, 2008, **20**(11), 1294–1299.
- 42 T. Luxbacher, Electrokinetic properties of natural fibres, in *Handbook of Natural Fibres*, Woodhead Publishing, 2020, pp. 323–353.
- 43 E. P. K. Currie, W. Norde and M. C. Stuart, Tethered polymer chains: surface chemistry and their impact on colloidal and surface properties, *Adv. Colloid Interface Sci.*, 2003, **100**, 205–265.
- 44 M. R. Esfahani, *Humic Acid Fouling on an Ultrafiltration Membrane: towards Nanocomposite-Based Self-Cleaning Membranes*, Doctoral dissertation, Tennessee Technological University, 2015.
- 45 E. J. Petersen, A. J. Kennedy, T. Hüffer and F. von der Kammer, Solving familiar problems: Leveraging environmental testing methods for nanomaterials to evaluate microplastics and nanoplastics, *Nanomaterials*, 2022, **12**(8), 1332.
- 46 M. C. Ariza-Tarazona, J. F. Villarreal-Chiu, J. M. Hernández-López, J. R. De la Rosa, V. Barbieri, C. Siligardi and E. I. Cedillo-González, Microplastic pollution reduction by a carbon and nitrogen-doped TiO<sub>2</sub>: Effect of pH and temperature in the photocatalytic degradation process, *J. Hazard. Mater.*, 2020, **395**, 122632.
- 47 W. Zhao, Z. Su, T. Geng, Y. Zhao, Y. Tian and P. Zhao, Effects of ionic strength and particle size on transport of microplastic and humic acid in porous media, *Chemosphere*, 2022, **309**, 136593.
- 48 X. Yang, G. Huang, X. Geng, L. Lyu, H. Bi and C. An, Deciphering the behavior and fate of microplastics in coastal aquatic environments: A comprehensive review illuminating coastal dynamics and driving mechanisms, *Earth-Sci. Rev.*, 2025, **270**, 105235.
- 49 S. Sharma and A. Bhattacharya, Drinking water contamination and treatment techniques, *Appl. Water Sci.*, 2017, **7**(3), 1043–1067.
- 50 J. Chen, J. Wu, P. C. Sherrell, J. Chen, H. Wang, W. X. Zhang and J. Yang, How to build a microplastics-free environment: strategies for microplastics degradation and plastics recycling, *Advanced Science*, 2022, **9**(6), 2103764.
- 51 S. Luederwald, J. Davies, T. F. Fernandes, A. Praetorius, J. A. Sergent, K. Tatsi, J. Tell, N. Timmer and S. Wagner, Practical considerations to optimize aquatic testing of particulate material, with focus on nanomaterials, *Environ. Sci.: Nano*, 2024, **11**(6), 2352–2371.

